Hindawi Publishing Corporation
International Journal of Antennas and Propagation
Volume 2012, Article ID 659287, 10 pages
doi:10.1155/2012/659287

Research Article

Snaps to Connect Coaxial and Microstrip Lines in Wearable Systems

Tiiti Kellomäki

Department of Electronics, Tampere University of Technology, P.O. Box 692, 33101 Tampere, Finland

Correspondence should be addressed to Tiiti Kellomäki, tiiti.kellomaki@iki.fi

Received 27 July 2012; Revised 27 September 2012; Accepted 2 November 2012

Academic Editor: Apostolos Georgiadis

Commercial snaps (clothing fasteners) can be used to connect a coaxial cable to a microstrip line. This is useful in the context of wearable antennas, especially in consumer applications and disposable connections. The measured *S*-parameters of the transition are presented, and an equivalent circuit and approximate equations are derived for system design purposes. The proposed connection is usable up to 1.5 GHz (10 dB return loss condition), and the frequency range can be extended to 2 GHz if a thinner, more flexible coaxial cable is used.

1. Introduction

Wearable antennas and sensors find their use in healthcare, rescue work, and recreation. In telemedicine scenarios the sensory information is transmitted from the patient to a physician or an automatic data processing system [1]. A wearable sensor would either transmit the information to the user's mobile phone via a low-power link, or directly to a base station. Positioning services can also be provided by wearable antennas. In the context of rescue work, firefighters and police officers need constant communication links. Wearable antennas can be easily integrated in their working outfits [2], and the radio equipment can then be placed in a designated pocket with RF (radio frequency) connectors to connect to the wearable antenna.

The recreational possibilities of wearable antennas are vast, for example, built-in satellite positioning systems in outdoor clothing or wearable sensors that communicate their data (acceleration, step count, skin temperature, and heart rate) to the user's mobile device, thus aiding in optimising athletes' training programmes. Such information can also be used purely for the purposes of entertainment or mutual competition among friends.

Example designs of wearable antennas include a variety of microstrip patch antennas [2], dipoles [3], and invertedF antennas [4]. The process flow of textile antenna design is described in [5]. Wearable sensors can be integrated in the clothing [6], or a sticking plaster can be used to attach the sensors to the skin [7]. Physiological signals to be measured with wearable sensors include, for example, heart rate or ECG, body temperature, and respiration [1].

In all the scenarios including wearable antennas and sensors, a radio transmitter/receiver is required. Presently it is not possible to include a washable radio in the clothing, but the equipment have to be disconnected when the clothes and the wearable antenna are washed. A natural choice would be to use a microstrip line or a stripline in the clothing and a flexible coaxial cable to connect the radio equipment to the microstrip. The connection between the coaxial and the microstrip lines must be simple so that the user is able to make the connections and disconnections unaided. Moreover, the connector in the clothing must withstand washing.

Common snap fasteners can be used to connect the coaxial and microstrip lines. The advantages of the snaps include washability, ease of use, and low cost. Snaps are also well known in the textile industry and thus require no extra machinery when smart clothing is manufactured. Snaps are available in a great variety of sizes and designs, from the robust and heavy snaps used in outdoor clothing to tiny snaps with a diameter of 3 mm used in doll clothes. Even the regular 9-volt battery design uses snaps, which are mechanically strong despite their small size (8 mm

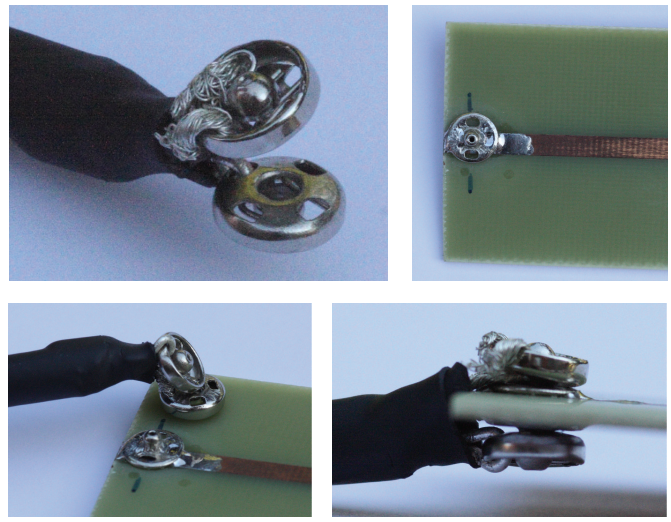

Figure 1: Photos of the transition (type A). Diameter of the snap is 7 mm.

diameter). Snaps can be sewn onto the fabric or attached by pressing through it. In the context of electronics, metallic snaps can be soldered on metals.

Naturally, a connection with snaps is not nearly as precise as special RF connectors. The frequency band of BNC connectors commonly extends to 4 GHz and SMA up to 18 GHz [8], but in this paper, it will be shown that the snaps are usable only up to 1.5–2 GHz. Most traditional RF connectors are quite large for wearable systems, although small snap-on surface mount connectors such as the U.FL are available [9]. However, RF connectors are much more expensive than snaps and not robust enough to withstand washing or the potential mishandling by the user (unaligned threads, rotation of the female connector, twisting, or breaking of the centre pin). This, especially the price, makes snaps an option worth considering in wearable antenna feeds.

In addition to the traditional use in clothing, snaps are widely used, for example, in healthcare: low-frequency signals of heartbeat are measured using plaster electrodes, which are then connected to the measurement instrument cables via snaps. Snap connectors have been used in the feeding arrangement of microstrip antennas in [10, 11]. Being cheap, snaps are especially handy in disposable connections, where the expensive coaxial cable can be reused.

Originally, the idea of using snaps in an RF connection was presented in [12], where the snaps were used to directly feed a microstrip antenna. Further measurements of snaps in a coaxial-to-microstrip transition were given in [13]. The present paper contains the full S-parameter measurement results, introduces a new geometry for comparison and experiments on the effect of the connection dimensions on the performance. Based on the measurement results, an equivalent circuit is presented along with equations that can be utilised as a block in system design.

This paper is structured as follows. The proposed transition geometry and the measurement setup are described in the next section. The results are presented in Section 3, where the effect of geometry changes is also investigated. Finally, the last section concludes the findings.

2. Snap Connection and Measurement Setup

The proposed snap transition structure consists of two male snaps attached (soldered) to the microstrip line, and the corresponding female snaps attached to the coaxial cable. One of the snaps is connected to the ground and the other to the signal conductor. Photographs of the proposed structure are shown in Figure 1.

Two transition geometries were studied, and the experiments were repeated using different snap sizes. In type A transition, the snaps are connected on both sides of the microstrip line with centres coinciding. Type B features the snaps on the same side of the PCB (printed circuit board), one after the other. Figure 2 shows the geometries. The male snaps were soldered directly on the PCB. The inner and outer conductors of the coaxial cable were threaded through the female snap sewing holes and secured by twisting. To prevent short circuiting, a short length of coaxial dielectric was left on the inner conductor, and heat-shrinkable plastic tubing was used over the outer conductor.

FR4 board and RG-142 coaxial cable were used in the test setups. In wearable consumer applications, the microstrip line would be fabricated on a textile substrate, but for the purposes of this paper, a well-known PCB was chosen to eliminate uncertainties caused by materials. The behaviour of snaps on a textile substrate has been investigated in [13], where they were found feasible. Long coaxial cables and microstrip lines were used because this allows separating the reflection caused by the transition from spurious echoes caused by the setup. Table 1 lists the key dimensions in the setup.

The snaps were commercial off-the-shelf snaps of Rei (7 mm snaps) and Prym (11 mm) trademarks. The Prym snaps are made of brass, with small amounts of nickel inside. There is no coating material. The material of the Rei snaps

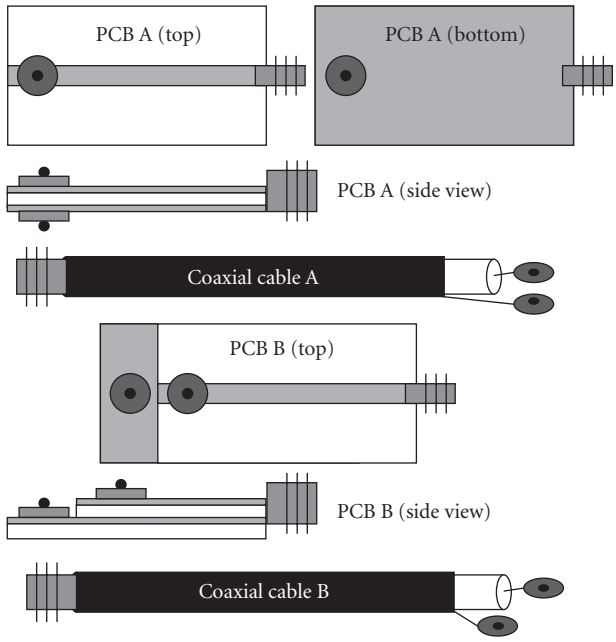

Figure 2: Geometry of the transition. Above: type A and below: type B. Drawings are not to scale.

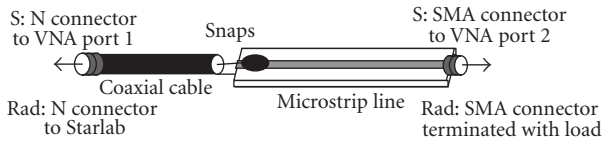

Figure 3: Measurement setup. S: in the *S*-parameter measurement, the connectors are connected to the VNA. Rad: in the radiation pattern measurement, the coaxial cable is connected to Satimo Starlab, and the microstrip is terminated with a matched load.

Table 1: Selected dimensions.

Microstrip thickness	1.6 mm
Microstrip line width	3 mm
Microstrip ground width	33 mm
Microstrip length	26–30 cm
PCB dielectric constant	4.4
Microstrip effective dielectric constant	3.3
Coaxial inner conductor diameter	0.95 mm
Coaxial dielectric diameter	2.95 mm
Coaxial dielectric constant	2
Coaxial length	16–25 cm
Snap diameter	7 and 11 mm
Distance between snap centres (type B)	1 cm

could not be verified; they are metallic, presumably also brass with no coating.

The measurement setup is shown in Figure 3. The *S*-parameters of the transition were measured using a vector network analyser (VNA). Multiple reflections from the snaps and the coaxial N/SMA adapters corrupt the raw measurement result of the complete setup. Also the attenuations and electrical lengths of the coaxial and microstrip lines are present in the raw result. To isolate only the reflection from the proposed snap structure, time-gating was used. The data are transformed from frequency domain to time domain by means of inverse Fourier transform. A temporal filter (gate) is used to reject other responses than the desired one. When the filtered data are transformed back to frequency domain, only the frequency response of the snap connection is present. This is illustrated in Figure 4. The VNA was calibrated using the SOLT (short-load-open-through) method. Because a narrow gate requires a wide frequency range, a frequency range of 50–6000 MHz was used.

Table 2: Measured insertion losses of the transmission lines in the setup.

	50 MHz	1 GHz	2 GHz
Microstrip	0.1 dB	0.4 dB	0.8 dB
Coaxial	0 dB	0.1 dB	0.1 dB

The electrical lengths and attenuations of the microstrip line and the coaxial cable were measured separately using a VNA. In this measurement, the lines were fed from the SMA end, and the snap end was terminated with a short circuit. The S_{11} of the short-circuited lines was then measured, and the attenuation was extracted from the result. Table 2 presents the insertion losses of the microstrip and coaxial lines. The electrical lengths of the lines were measured in time domain.

For the purposes of the actual *S*-parameter measurement, port extensions (phase shift) were programmed for each of the VNA ports, thus moving the reference planes to the end of the coaxial outer conductor and at the centres of the snaps on the PCB, as illustrated in Figure 5. This compensates for the electrical lengths of the coaxial and microstrip lines. The attenuations of the lines were subtracted from the results in postprocessing. Thus, only the *S*-parameters of the snap connection are visible in the final results presented in this paper.

The radiation from the snap structure was measured with Satimo Starlab [14] from 800 MHz to 3 GHz. In this measurement the coaxial cable was connected to the feed port in Starlab, and the microstrip line was terminated using a 50-ohm load (see Figure 3). The measurement results of the radiation from the transition include the effect of the complete measurement setup: the coaxial adapters, the coaxial cable, the snaps, the microstrip line, and the termination. To make the setup fit inside Starlab, the snap connection was bent during the radiation measurement (see Figure 12), and thus the radiation measurements will show a worst case situation.

3. Results

The measured *S*-parameters are first presented for type A transition with 7 mm diameter snaps. An equivalent circuit representation will be introduced. The difference between transition geometries (types A and B) is investigated as well

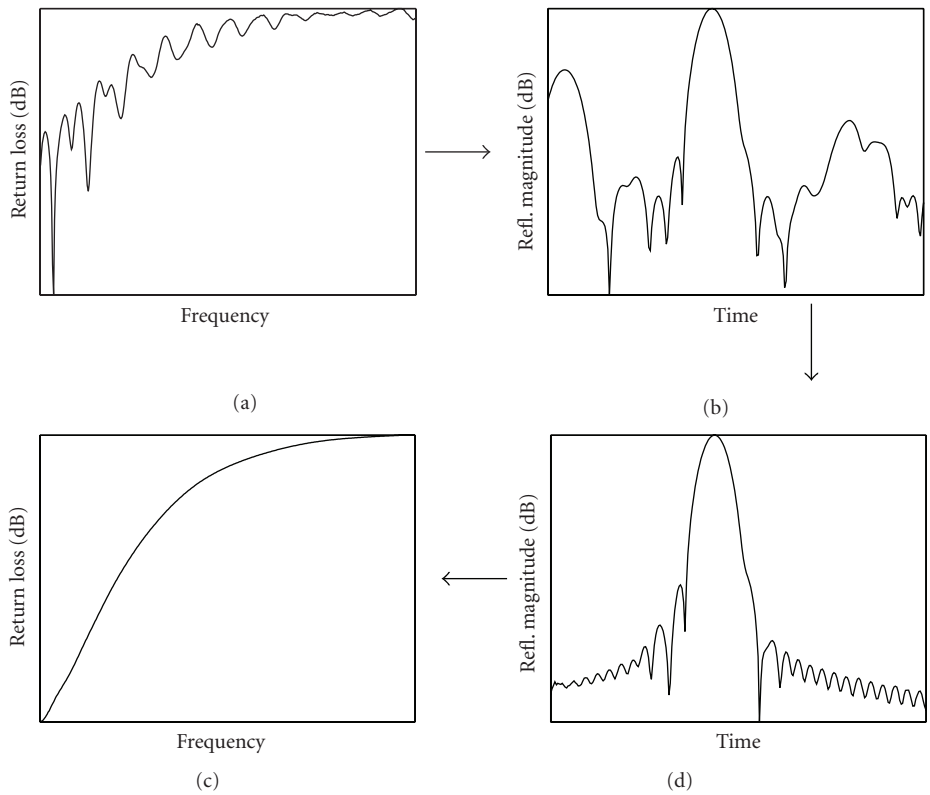

Figure 4: Principle of gating. (a) Return loss of the system in frequency domain corrupted with multiple reflections from the RF connectors on the coaxial and the microstrip lines. (b) Time-domain response of the system acquired by inverse Fourier transform of the frequency-domain response. (c) When gating is applied to the time-domain response, only the desired echo remains. (d) By applying Fourier transform, the uncorrupted frequency response is found.

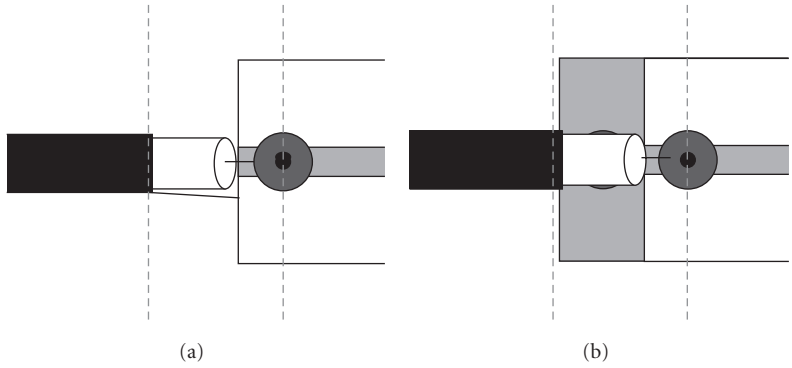

Figure 5: Reference planes for the S-parameter measurement. (a) type A and (b) type B.

as the effect of snap sizes and coaxial cable thickness. The repeatability of the connection will be studied. Finally, an example of using the transition is given: snaps in antenna feed.

3.1. S-Parameters and Radiation of the Transition. The measured S-parameters of the transition (type A with 7 mm snaps) are presented in Figure 6. The input return loss remains better than 10 dB until 1.65 GHz and output return loss until 1.5 GHz. The insertion loss is small, −0.7 dB at 1.5 GHz.

The losses were calculated from the S-parameters: efficiency = $(|S_{11}|^2 + |S_{21}|^2) \cdot 100\%$. In the range from 0 to 1.8 GHz, the efficiency stays above 90%. Most of the power loss is due to radiation from the transition; the measured antenna efficiency of the transition is 6% at 1.8 GHz. The measured radiation from the complete system is given in Figure 7 (thick coax). Up to 1.5 GHz the radiation loss is relatively low, but then it starts to increase rapidly.

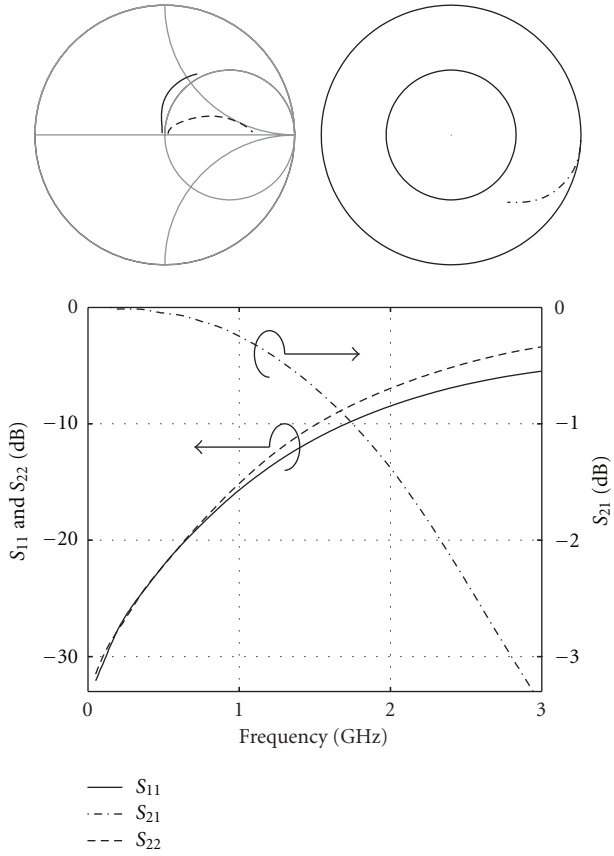

Figure 6: Measured S-parameters of the transition, type A, 7 mm snaps.

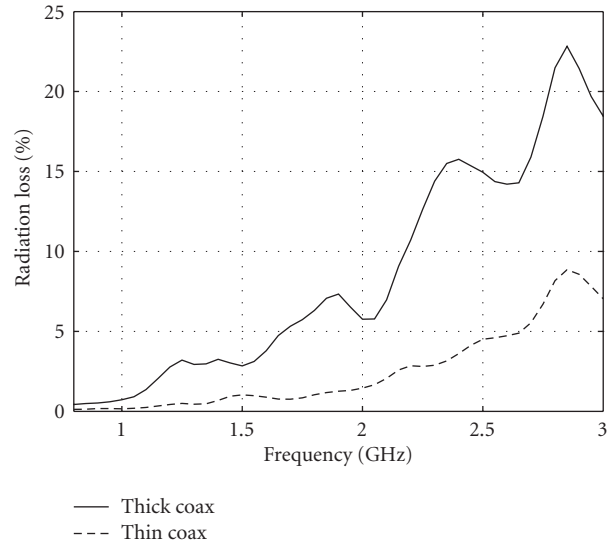

Figure 7: Measured radiation loss of the transition (type A, 7 mm snaps). The vertical axis shows the ratio (power radiated from system)/(power available from source), that is, power lost from the transition in the form of radiation. Radiation from the microstrip line and other parts of the setup has not been removed, and line attenuations have not been deembedded. Undulation in the curve is due to impedance mismatch in the transition.

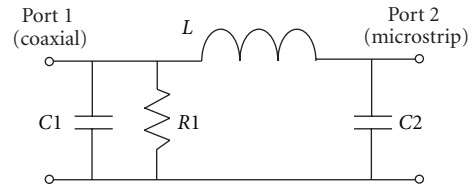

Figure 8: Equivalent circuit.

The physical length of the transition is approximately 1 cm. In the range from 0 to 1500 MHz, the measured delay was 46 ps. This corresponds to 1 cm of propagation with a velocity of 0.74 times the speed of light or with an effective dielectric constant of 1.8. Compared to transmission on the coaxial cable or the microstrip line of the same physical length, positive phase is introduced. In other words, the snap transition is electrically shorter than a microstrip or a coaxial line of the same length.

The DC resistance of the transition was also measured and found to be of the order of milliohms. This means that the electrical connection does not pose a problem.

3.2. Equivalent Circuit and Approximate Equations. The transition can be modelled as a π topology lowpass filter with two parallel capacitors and one series inductor, with some losses added in the form of a parallel resistor. This topology has been used, for example, in [15]. The circuit model is presented in Figure 8. Constant component values usable up to 1.5 GHz are given in the first column of Table 3. The circuit exhibits a large series inductance due to the long transition structure, which makes the transition reflective at relatively low frequencies. For comparison: Majewski presents $L = 0.2\,\text{nH}$, $C1 = 0.2\,\text{pF}$, and $C2 = 0.02\,\text{pF}$ and no parallel resistance (i.e., infinite value) for a standard SMA connector at the edge of a PCB [15].

Figure 9 illustrates the validity of the equivalent circuit. The S_{21} of the equivalent circuit is within ± 0.2 dB of the measured value up to 1.5 GHz and within ± 1 dB until 2 GHz. S_{11} and S_{22} deviate from the measured values by ± 1 dB at the maximum until 2.7 GHz.

The main difference between the S-parameters of the equivalent circuit and the measured response is the phase angle of S_{21}; the delay is overestimated by the lumped component model. At 1.5 GHz, the phase should be only -35°, while the model gives -61°. The equivalent circuit slightly overestimates the frequencies, where the return losses at each port cross 10 dB by 130 MHz at port 2 and by 60 MHz at port 1.

In terms of the magnitude of the S-parameters, the equivalent circuit model is usable from DC to 2 GHz (error max. 1 dB). However, if accurate phase characteristics are needed, only the range from DC to 1 GHz is covered by the model (phase error max. 20°).

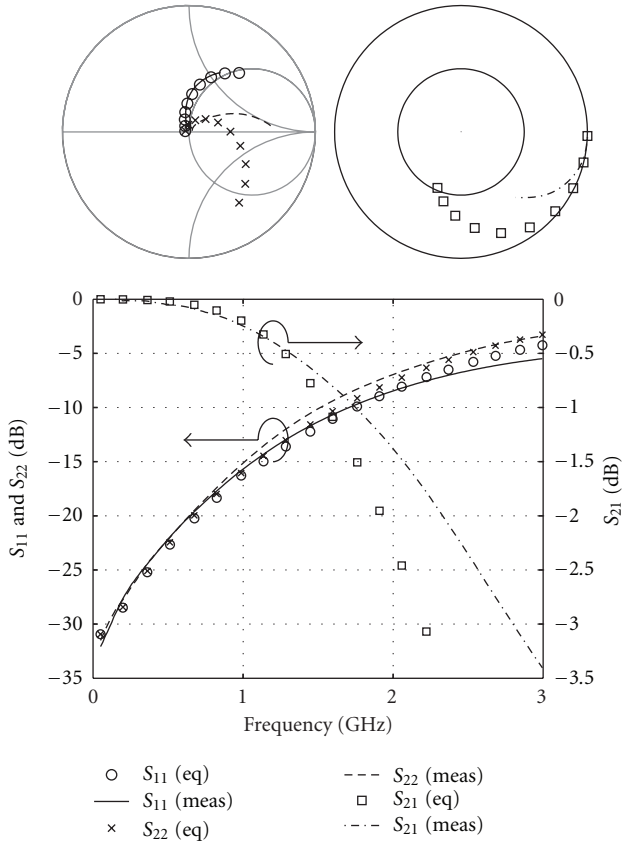

Figure 9: S-parameters of the equivalent circuit compared to the measured results (type A, 7 mm).

The S-parameters can also be quite accurately represented by simple equations:

$$
\begin{aligned}
|S_{11}| &= 0.194f - 0.011,\\
\angle S_{11} &= -19.353f + 118.110,\\
|S_{21}| &= -0.042f^2 + 0.009f + 1.002,\\
\angle S_{21} &= -16.666f - 1.705,\\
|S_{22}| &= 0.245f - 0.041,\\
\angle S_{22} &= -18.638f + 55.986,\\
S_{12} &= S_{21},
\end{aligned}
\tag{1}
$$

with the frequency f in GHz. The equations give the magnitude in linear units and angle in degrees.

Using the equations results in ±1 dB error in S_{11} and S_{22} up to 3 GHz and ±0.2 dB error in S_{21}. Above 500 MHz, the phase angles given by the equations are within 2° of the measured values. Below 500 MHz, the phase angles of S_{11} and S_{22} are given incorrectly, but because the magnitudes are very small, this is not a problem. The phase of S_{21} as given by the equation stays within 2° of the measured value from 0 to 3 GHz. Thus, the equations are valid from DC to 3 GHz.

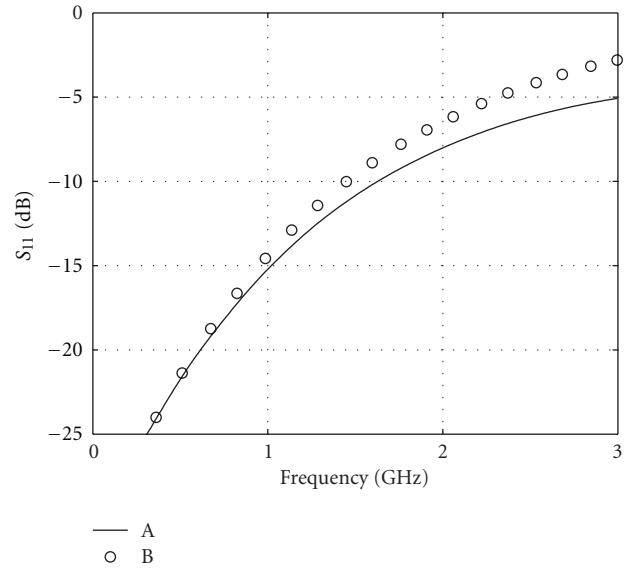

Figure 10: Measured input reflection coefficient of transition types A and B, both with 7-mm snaps.

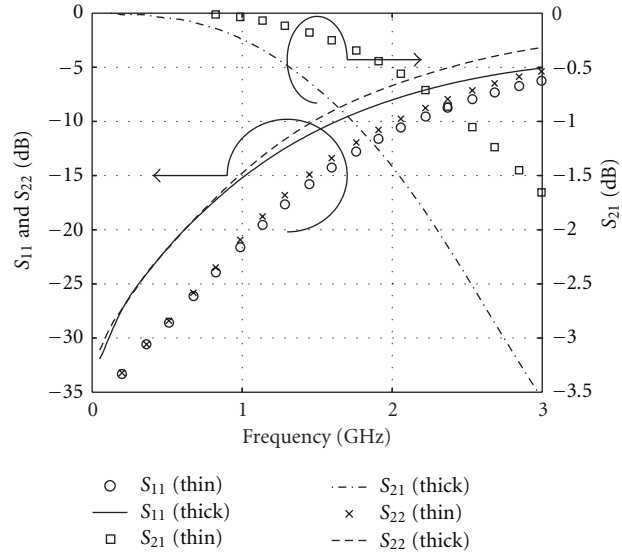

Figure 11: S-parameters of the transition measured with thin and thick coaxial cables (type A, 7 mm).

3.3. Difference between Transition Types A and B. In the transition geometry B, the snaps are on the same side of the PCB, one after the other, as shown in Figure 2. The centres of the snaps are approximately 1 cm away from each other (with snap diameter 7 mm), and thus type B transition is longer than type A. This type of a transition may be easier to fabricate in some applications, and thus it is worth experimenting with.

According to the measurements, type A performs slightly better than type B. The input return loss of type B transition crosses 10 dB at 1.45 GHz, whereas for type A only at 1.63 GHz. Figure 10 shows how the matching of type A transition is better especially at higher frequencies.

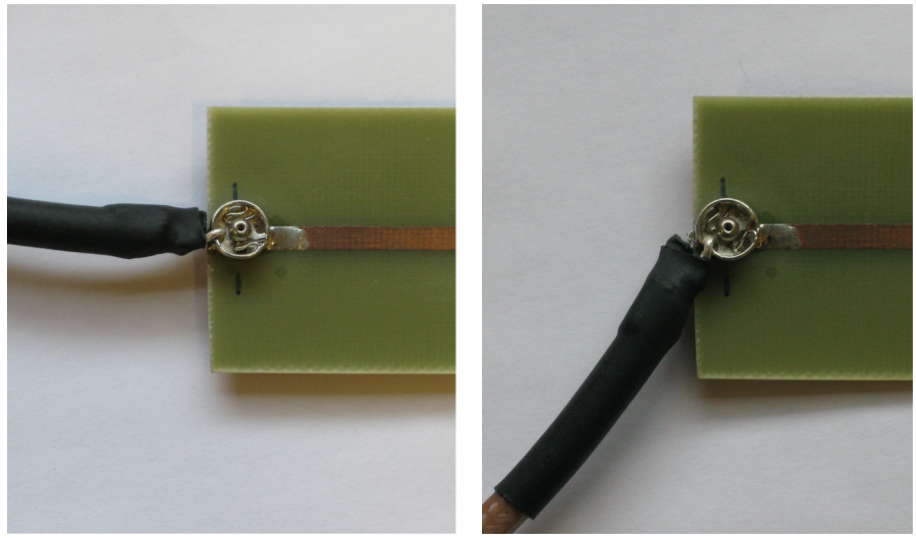

(a) (b)

Figure 12: Testing the repeatability of one connection. The coaxial cable was reattached eight times, both in a straight (a) and a bent configuration (b).

Table 3: Component values for the equivalent circuit with snap diameter 7 mm.

	type A	type B	type A, thin coax
L	5.1 nH	5.3 nH	3.1 nH
C1	0.2 pF	0 pF	0 pF
C2	1 pF	1 pF	1 pF
R1	880 ohm	880 ohm	1700 ohm

The transmission and S_{22} characteristics are virtually the same for both transition types. The total losses in both of the transition geometries are approximately the same.

To make the equivalent circuit match type B transition, the inductance value must be increased because of the physically longer structure, and the input capacitance must be removed altogether (0 pF). The equivalent circuit parameters for transition type B are given in the second column of Table 3.

3.4. Effect of Snap Size and Coaxial Thickness. When larger (11-mm) snaps are used, the length of the transition increases. This was believed to add more inductance and thus to lower the 10-dB return loss frequency. However, there was virtually no effect on the frequency range. The same component values in the equivalent circuit can be used for both 7-mm and 11-mm snaps. This leads us to believe that any snaps of a reasonable size could be used in the structure.

The inner conductor of the RG-142 coaxial cable used in our prototyping is solid and 0.95 mm thick, which makes it almost too rigid for twisting around the sewing hole of a snap. With small (6 mm) snaps, the connection was very unreliable because of the thick conductor. As seen from the photographs in Figure 1, the snaps are easily unfastened by the torque from the conductor threads that pass between the snap and the microstrip line. The mechanical robustness of the connection is a problem that needs attention before consumer-grade applications of snaps can emerge.

Using a thinner coaxial cable with a thinner centre conductor makes it easier to fabricate the transition. The measurements were repeated using a no-brand coaxial with a braided 0.6 mm (diameter) inner conductor and 1.6 mm dielectric. In addition to being much easier to fabricate, the transition also performed better than the thick coaxial counterpart, which is clear from Figure 11.

The return losses of the transition with a thin coaxial cable stayed below 10 dB until 2 GHz. As calculated from the *S*-parameters, the losses in the transition were 5–10% lower with the thin cable than the thick one (measured up to 2 GHz). The result is consistent with the measured radiation; approximately 0.15% of the power was radiated from the system at 1 GHz and 1.5% at 2 GHz, which is considerably lower than from the transition with a thick cable. The radiation loss is illustrated in Figure 7.

Using the thinner cable results in a shorter connection, because the inner conductor can be much more easily threaded in the snap holes. A 10–15 ps delay was measured, which is considerably smaller than the 46 ps measured for type A transition with the thick cable. The equivalent circuit matches the measurement results when the component values are brought towards ideal; the inductance decreased, input capacitance removed, and input parallel resistance increased, as given in the third column of Table 3.

3.5. Repeatability. Both the repeatability of the connection and the repeatability in fabricating a set of snap connectors were examined. The first test was done simply by attaching and reattaching one connection between measurements. This was done eight times. For the other test, two coaxial

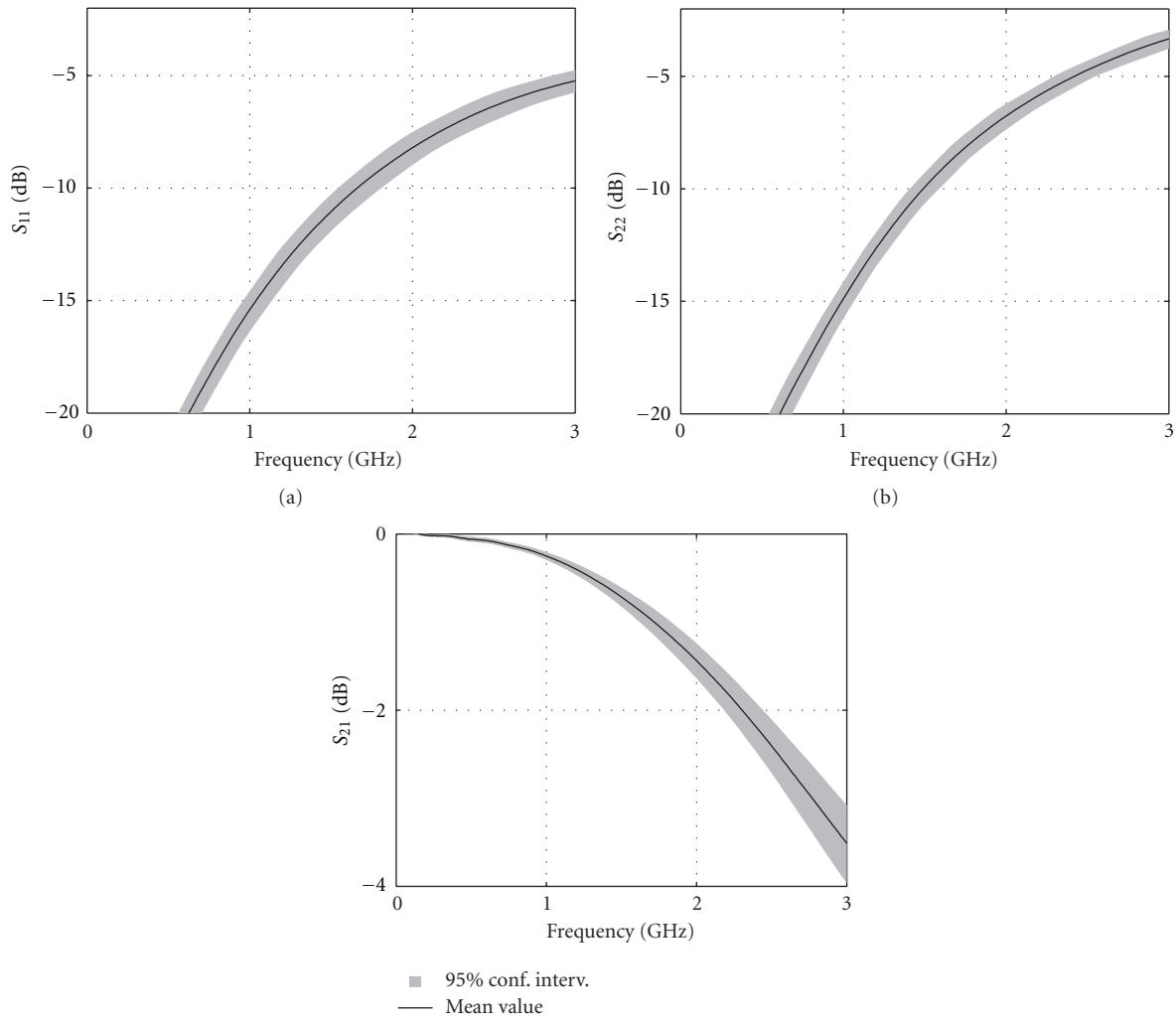

Figure 13: Repeatability of one connection (type A, 7 mm). The shaded area indicates the calculated interval in which 95% of connections will fall.

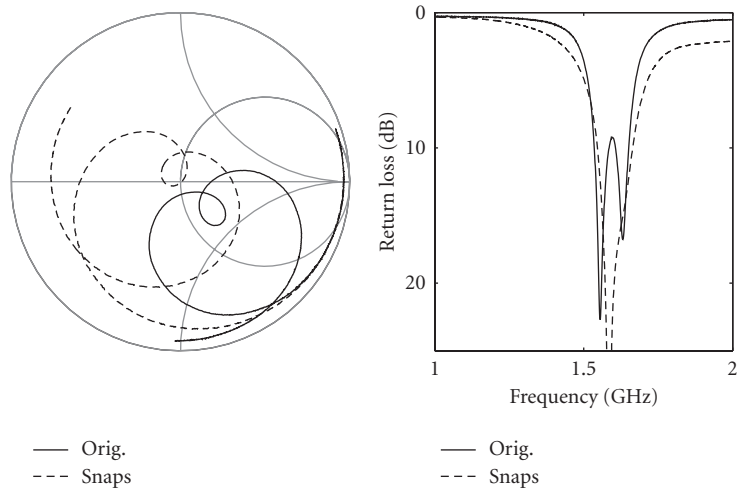

Figure 14: Calculated input impedance of an antenna fed using the transition (type A, 7 mm).

Table 4: Observed variation in S-parameters around the mean value when one connection is repeated or multiple connections are fabricated and measured. Data for S_{11} and S_{22}:750 to 2500 MHz. Data for S_{21}:0 to 2500 MHz. The last row indicates changes in the frequency, where either one of the return losses crosses 10 dB.

	Repeated connection (straight)	repeated connection (bent)	fabrication
S_{11}	±0.5 dB	±0.8 dB	±1.5 dB
S_{22}	±0.6 dB	±0.7 dB	N/A
S_{21}	±0.2 dB	±0.3 dB	±0.2 dB
f_{10} dB	±80 MHz	±120 MHz	±200 MHz

cables and two microstrip lines were fabricated (type A, 7 mm), and each of the four pairs was measured.

Generally, the repeatability of S_{11} and S_{22} becomes better with increasing frequency, whereas S_{21} is more repeatable in the lower frequency range. The lowest frequencies (0 to 750 MHz) are excluded from the following analysis of S_{11} and S_{22}, because the reflection coefficients are very small, and any deviation results in a huge relative difference.

When one connection was repeated with the same cable and microstrip, very small changes were seen in the measured S-parameters. The repeatability was tested both with a straight and a bent configuration, which are illustrated in Figure 12. The bent configuration introduced more variation in the results, but still the repeatability was quite good. Table 4 summarises the observations.

The repeated measurements were analysed statistically. When the data are assumed normally distributed (with a different mean and variance at each frequency), it is possible to give the 95% confidence interval, that is, the interval in which the S-parameters of 19 out of 20 connections will fall. Figure 13 shows the mean values, the 95% confidence intervals, and the measured values. Based on the data in the figure, the upper limit of the usable frequency band is estimated to vary from 1400 to 1600 MHz.

The different fabricated prototypes were similar in terms of S_{21}. The observed differences are ±1.3 dB in S_{11} at 1.5 GHz and ±1 dB at 2 GHz. The frequency where the return loss crosses 10 dB varied between 1600 and 1900 MHz, or ±200 MHz around the mean value, from cable to cable. Fabrication tolerances are the major source of variation in the hand-made connections, but with machine assembly, it is possible to manufacture samples more alike. Thus, the main concern in commercial applications would be the repeatability of one connection.

3.6. Example: Antenna Impedance through the Transition. Figure 14 shows the input impedance of an antenna fed using the proposed transition structure. The antenna is a circularly polarised detached-corner microstrip patch antenna published in [16] and constructed on a flexible textile substrate. Some dimensions of the antenna are given in Table 5. The data in Figure 14 are acquired by computing the input reflection coefficient of the snap transition and the antenna in a cascade connection. At this frequency, the antenna efficiency would be lowered by 0.8 dB or 17% because of the losses and reflections in the snap connection.

Table 5: Dimensions of the antenna fed with the snap connection in the example.

Element width and length	60.8 mm
Substrate thickness	1.3 mm
Ground plane width and length	121.6 mm
Feed inset	2 mm
Feed line width	3.5 mm
Substrate dielectric constant	2.4

With the help of the S-parameters presented in this paper, it is possible to design antennas whose impedance matches the output impedance of the snap connection. The snaps can then be viewed as a matching circuit for the antenna. With proper matching, only the ohmic (and possible radiation) losses in the connection would lower the antenna efficiency. For example, if the matching of the antenna described in this section was redesigned, the connection would lower the efficiency by only 0.4 dB (8%).

4. Conclusion

The S-parameters of a coaxial-to-microstrip transition using commercially available sewing snaps have been presented, along with an equivalent circuit and approximate equations for the frequency response. The proposed transition can be used from DC to 1.4 GHz, according to the condition of return losses >10 dB. With a thinner coaxial, the transition can be made shorter, which increases the frequency range to 2 GHz. Thin, flexible coaxial cables will also be more comfortable to the user. According to preliminary studies, the repeatability of the connection is of the order of ±1 dB for return losses and 0.2 dB for transmission in the frequency range from 750 to 2000 MHz.

Two transition geometries were studied: one with the snaps on both sides of the microstrip line with centres coinciding and the other with the snaps on one side of the PCB one after the other. While the former one performs slightly better, the latter can also be used if the application demands this kind of a structure.

In the prototypes, the snaps were connected to the coaxial cable by means of twisting the conductors around the snap holes. This way the conductor must also pass below the snap, between the snap and the microstrip line. This makes the contact surface uneven, as seen in Figure 1, and the snaps are also easily unfastened by the torque. If press-on snaps were used instead of sew-on snaps, the threads would pass inside the snap, and thus the robustness of the connection could be improved. More robust snaps can be used also in the electrical connection, such as those in a 9-volt battery. Additionally, an extra snap with good mechanical attachment properties (such as those used in outdoor clothing) could be used to fasten the plastic cover of the coaxial cable to the garment. If the cable becomes twisted or pulled, the strong snap would keep the connection

in place, and no torque would be applied to the small snaps responsible for the electrical connection. Future work is needed to create a stable connection.

Compared to traditional RF connectors, the snaps perform poorly. For example, the typical return loss of an SMA connector is 29 dB, N connector is 27 dB, and MMBX is 26 dB at 2.5 GHz [8], while the return loss of the snaps is already 10 dB at approximately 1.5 GHz. The advantages of the snaps lie in the simple structure: the snap connection is easy to use, the snaps are small and washable, and the connection is cheap. Compared to snap-on type RF connectors (SMB, MCX, or U.FL), clothing snaps fasteners are at least 20 times cheaper.

The snaps are applicable for consumer applications in relatively low frequencies, such as broadcast radio (100 MHz), GPS or Galileo positioning systems (below 1600 MHz), radio frequency identification (850–900 MHz), and industrial-scientific-medical applications near 430 or 900 MHz. The power rating of the snap transition has not been accessed. For now, we recommend using the transition in receiving systems or lowpower transmission systems only.

Acknowledgment

This work was funded by the Finnish Cultural Foundation, Pirkanmaa Regional Fund.

References

[1] W. Scanlon and N. Evans, "Antennas and propagation for telemedicine and telecare: on-body systems," in *Antennas and Propagation for Body-centric Wireless Communications*, P. S. Hall and Y. Hao, Eds., chapter 8, pp. 211–239, Artech House, 2006.

[2] L. Vallozzi, P. Van Torre, C. Hertleer, H. Rogier, M. Moeneclaey, and J. Verhaevert, "Wireless communication for firefighters using dual-polarized textile antennas integrated in their garment," *IEEE Transactions on Antennas and Propagation*, vol. 58, no. 4, pp. 1357–1368, 2010.

[3] T. Kellomaki, J. Heikkinen, and M. Kivikoski, "Wearable antennas for FM reception," in *Proceedings of the European Conference on Antennas and Propagation (EuCAP '06)*, Nice, France, November 2006.

[4] J. Heikkinen, T. Laine-Ma, A. Ruhanen, and M. Kivikoski, "Flexible antennas for GPS reception," in *Proceedings of the European Conference on Antennas and Propagation (EuCAP '06)*, Nice, France, November 2006.

[5] P. Salonen and Y. Rahmat-Samii, "Wearable antennas: advances in design, characterization, and application," in *Antennas and Propagation for Body-centric Wireless Communications*, P. S. Hall and Y. Hao, Eds., chapter 6, pp. 151–188, Artech House, 2006.

[6] J. Rantanen, T. Vuorela, K. Kukkonen, O. Ryynänen, A. Siili, and J. Vanhala, "Improving human thermal comfort with smart clothing," in *Proceedings of the IEEE International Conference on Systems, Man and Cybernetics*, vol. 2, pp. 795–800, October 2001.

[7] T. Vuorela, J. Hannikainen, and J. Vanhala, "Plaster like physiological signal recorder—design process, lessons learned," in *Proceedings of the Ambience 08 Smart TextilesTechnology and Design*, Borås, Sweden, June 2008.

[8] Huber and A. G. Suhner, *RF Coaxial Connectors General Catalogue*, 2007.

[9] Hirose Electric Japan, "Ultra small surface mount coaxial connectors—1.9mm or 2.4mm mated height," 2012, http://www.hirose.co.jp/cataloge%20hp/e32119372.pdf.

[10] T. Kellomäki, W. G. Whittow, J. Heikkinen, and L. Kettunen, "2.4 GHz plaster antennas for health monitoring," in *Proceedings of the 3rd European Conference on Antennas and Propagation (EuCAP '09)*, pp. 211–215, Berlin, Germany, March 2009.

[11] T. Kellomäki and W. G. Whittow, "Bendable plaster antenna for 2.45 GHz applications," in *Proceedings of the Loughborough Antennas and Propagation Conference (LAPC '09)*, pp. 453–456, Loughborough, UK, November 2009.

[12] I. Belov, M. Chedid, and P. Leisner, "Investigation of snap-on feeding arrangements for a wearable UHF textile patch antenna," in *Proceedings of the Ambience 08 Smart TextilesTechnology and Design*, Borås, Sweden, June 2008.

[13] T. Kellomäki, "Snap-on buttons in a coaxial-to-microstrip transition," in *Proceedings of the Loughborough Antennas and Propagation Conference (LAPC '09)*, pp. 437–440, Borås, Sweden, November 2009.

[14] Satimo, September 2012, http://www.satimo.com/.

[15] M. L. Majewski, R. W. Rose, and J. R. Scott, "Modeling and characterization of microstrip-to-coaxial transitions," *IEEE Transactions on Microwave Theory and Techniques*, vol. 29, no. 8, pp. 799–805, 1981.

[16] J. J. Heikkinen, T. T. Laine-Ma, and M. A. Kivikoski, "Flexible fabric-base patch antenna with protective coating," in *Proceedings of the IEEE Antennas and Propagation Society International Symposium*, pp. 4168–4171, June 2007.